Inorganica Chimica Acta 427 (2015) 248–258

Contents lists available at ScienceDirect

Inorganica Chimica Acta

journal homepage: www.elsevier.com/locate/ica

Synthesis, characterization, *cis*-ligand substitution and catalytic alkane hydroxylation by mononuclear nickel(II) complexes stabilized with tetradentate tripodal ligands

Dattaprasad D. Narulkar, Amit R. Patil, Chandan C. Naik, Sunder N. Dhuri *

Department of Chemistry, Goa University PO, Taleigao Plateau, Panaji 403206, Goa, India

ARTICLE INFO

Article history:
Received 25 October 2014
Received in revised form 23 December 2014
Accepted 5 January 2015
Available online 12 January 2015

Keywords:
Nickel
N,N′-bis(8-quinolyl)ethane-1,2-diamine
N,N′-dimethyl-*N,N′*-bis(8-quinolyl)ethane-1,2-diamine
Crystal structure
ESI-mass spectra
Hydroxylation

ABSTRACT

The synthesis and spectroscopic characterization of the mononuclear complexes $[Ni(bqenH_2)(H_2O)_2](ClO_4)_2$ **1** and $[Ni(bqenMe_2)(H_2O)_2](ClO_4)_2$ **2** (where $bqenH_2$ = *N,N′*-bis(8-quinolyl)ethane-1,2-diamine and $bqenMe_2$ = *N,N′*-dimethyl-*N,N′*-bis(8-quinolyl)ethane-1,2-diamine) is reported. The $bqenMe_2$ ligand was prepared by a simple modification to the earlier procedure. The reaction of **1** and **2** with 1,10-phenanthroline (phen) or 2,2′-bipyridine (bpy) resulted in the formation of $[Ni(bqenH_2)(phen)](ClO_4)_2$ **3**, $[Ni(bqenMe_2)(phen)](ClO_4)_2$ CH_3CN **4**, $[Ni(bqenH_2)(bpy)](ClO_4)_2$ **5**, and $[Ni(bqenMe_2)(bpy)](ClO_4)_2$ **6**. The redox properties of **1**–**6** are reported. The crystal structures of **3** and **4** consist of distorted octahedral $[Ni(bqenH_2)(phen)]^{2+}$ and $[Ni(bqenMe_2)(phen)]^{2+}$ cations which are stabilized by N–H···O and C–H···O interactions. Compounds **1** and **2** afforded hydroxylation of alkanes with high alcohol to ketone ratio in the presence of *m*-CPBA oxidant.

1. Introduction

In biomimetic chemistry, the metal complexes are designed such that they resemble the active parts of metalloenzymes and correlate their structure–function relationship [1]. Several reports on nonheme metal complexes are available, especially of the first-row transition metals such as manganese [2–5], iron [6–11], copper [12–14] and cobalt [15] in their high valent metal-oxo, peroxo, superoxo forms and play crucial roles in the organic oxygenation reactions. The nickel metal is not an exception to this list, as a large number of nickel complexes with tripodal ligands such as tris(2-pyridylmethyl)amine (TPA), *N*-tetramethylated cyclam (*n*-TMC), *N*,*N*-dimethyl-*N′*,*N′*-bis(pyridin-2-ylmethyl)ethane-1,2-diamine (*iso*-BPMEN), *N*,*N*-dimethyl-*N′*,*N′*-bis(quinolin-2-ylmethyl)ethane-1,2-diamine (*iso*-BQMEN) are known (Scheme 1) [16–20]. In high valent nickel chemistry, the reactive nickel-dioxygen species such as nickel-superoxo, peroxo, acyl/alkyl peroxo are all well characterized [16–21]. The putative nickel-oxygen species (Ni^{III}=O or Ni^{II}–O) for the catalytic hydroxylation of alkanes using *m*-CBPA (*m*-chloroperbenzoic acid) has also been proposed in the literature [20–24].

The applications of nickel complexes are not exclusively limited to the chemical science and biomimetic fields, but vitally important in the different branches of biological sciences. A wide range of nickel complexes are known to exhibit an antioxidant and antimicrobial activity against the several microorganisms [25,26]. The nickel complexes of 1,10-phenanthroline (phen) and 2,2′-bipyridine (bpy) derivatives have shown the binding and cleavage of DNA residues [27–31]. Thus tuning the properties of metal complexes using an appropriate nonheme ligand architecture has become an art for the inorganic chemist from the days of Alfred Werner. Inspired by the versatility of nickel complexes and their applications in various fields especially in the organic oxidative transformations, here we focus on the synthesis of new Ni(II) compounds namely $[Ni(bqenH_2)(H_2O)_2](ClO_4)_2$ **1** and $[Ni(bqenMe_2)(H_2O)_2](ClO_4)_2$ **2** containing the tetradentate tripodal N4 ligands *N,N′*-bis(8-quinolyl)ethane-1,2-diamine ($bqenH_2$) and *N,N′*-dimethyl-*N,N′*-bis(8-quinolyl)ethane-1,2-diamine ($bqenMe_2$) respectively (Fig. 1).

The reactivity of **1** and **2** with 1,10-phenanthroline (phen) and 2,2′-bipyridine (bpy) has been investigated for the formation of compounds **3**–**6** (Fig. 1). Spectroscopic characterization, redox properties, crystal structure determination of **3** and **4** have been carried out. To probe the efficacy of synthesized compounds **1**–**6** for alkane hydroxylation, the catalytic oxidation of alkanes using

* Corresponding author. Tel.: +91 832 6519318.
E-mail address: sndhuri@unigoa.ac.in (S.N. Dhuri).

http://dx.doi.org/10.1016/j.ica.2015.01.009
0020-1693/

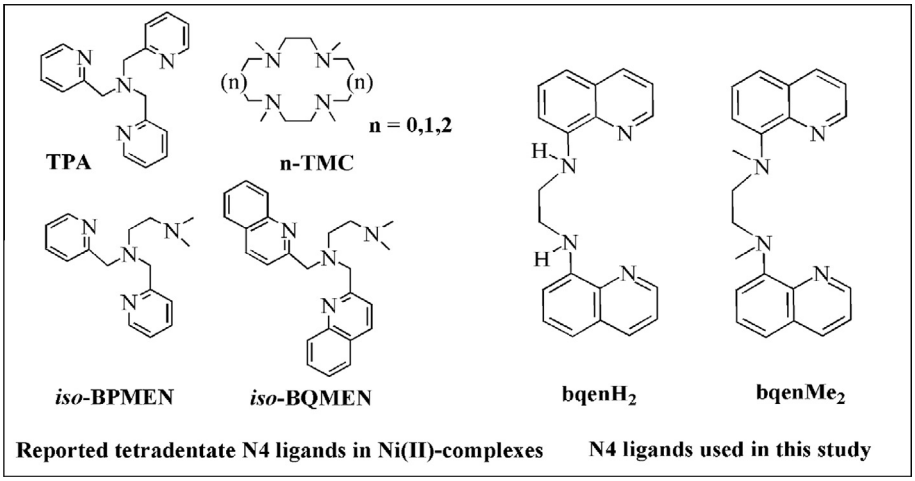

Scheme 1. Chemical structures of tetradendate tripodal ligands.

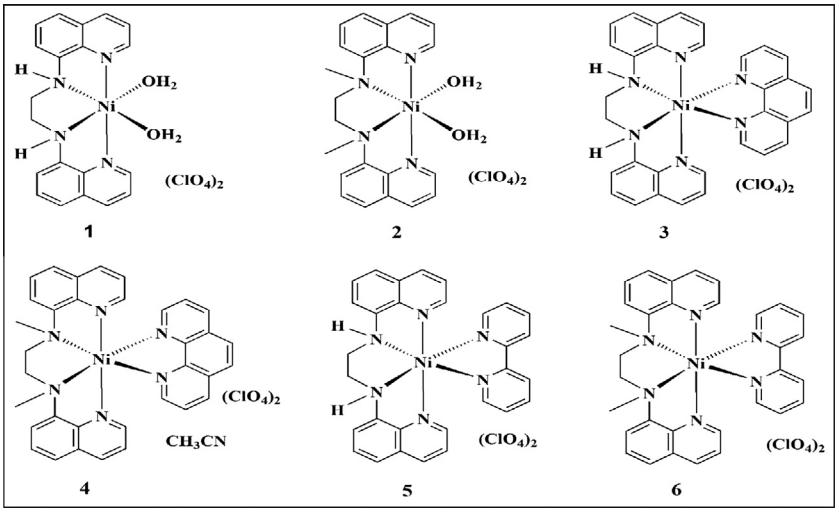

Fig. 1. Chemical structures of compounds **1**–**6**.

m-chloroperbenzoic acid (*m*-CPBA) as an oxidant has been studied. The results of these investigations are described in this paper.

2. Experimental details

2.1. Materials and methods

All the chemicals used in this study were purchased from commercial sources. The solvents were dried and distilled prior to use under the Ar or N_2 atmosphere. Elemental analysis was carried out on Elementar Variomicro Cube CHNS Analyser. Electrospray ionization mass (ESI-MS) spectra were measured on Thermo Finnigan (San Jose, CA, USA) LCQ™ Advantage MAX quadrupole ion trap instrument, by infusing samples directly into the source at 20 μL/min using a syringe pump. The spray voltage was set at 4.7 kV and the capillary temperature at 240 °C. The UV–Vis spectra were recorded in CH_3CN in the range 200–1100 nm using Agilent diode array 8453 UV–Vis spectrophotometer. The compounds were diluted in KBr powder and the infrared (IR) spectra were recorded in the region of 4000–400 cm^{-1} using Shimadzu (IR Prestige-21) FT-IR spectrometer. The ^1H and ^{13}C NMR spectra were recorded in $CDCl_3$ on Bruker Avance III 400 MHz NMR spectrometer. The cyclic voltammograms (CV) and differential pulse voltammograms (DPV) were recorded using Electrochemical Workstation-CH Instrument, Inc. CHI6107. A glass vessel containing sample solution was equipped with three-electrodes namely a platinum working electrode, platinum wire as counter electrode and standard calomel electrode as reference electrode. The experiments were carried in DMSO containing 0.1 M tetrabutylammonium hexafluorophosphate ($TBAPF_6$) as a supporting electrolyte and the solutions were purged with N_2 gas for around ~30 min prior to the each measurement. The single crystals of **3** and **4** suitable for X-ray studies were picked up and mounted directly on a Bruker SMART AXS diffractometer equipped with Mo Kα = 0.71073 Å radiation. The CCD data were integrated and scaled using Bruker-SAINT software package while SHEXTL V 6.12 was used for solving and refining the structures [32]. The non-hydrogen atoms were refined with the anisotropic displacement parameters while the hydrogen atoms were located at the calculated positions. In the catalytic oxidation reactions, the organic product analyses were carried out using Agilent Technologies 6890 N gas chromatograph (GC). The retention time and peak areas of the products were compared with authentic samples using decane as an internal standard.

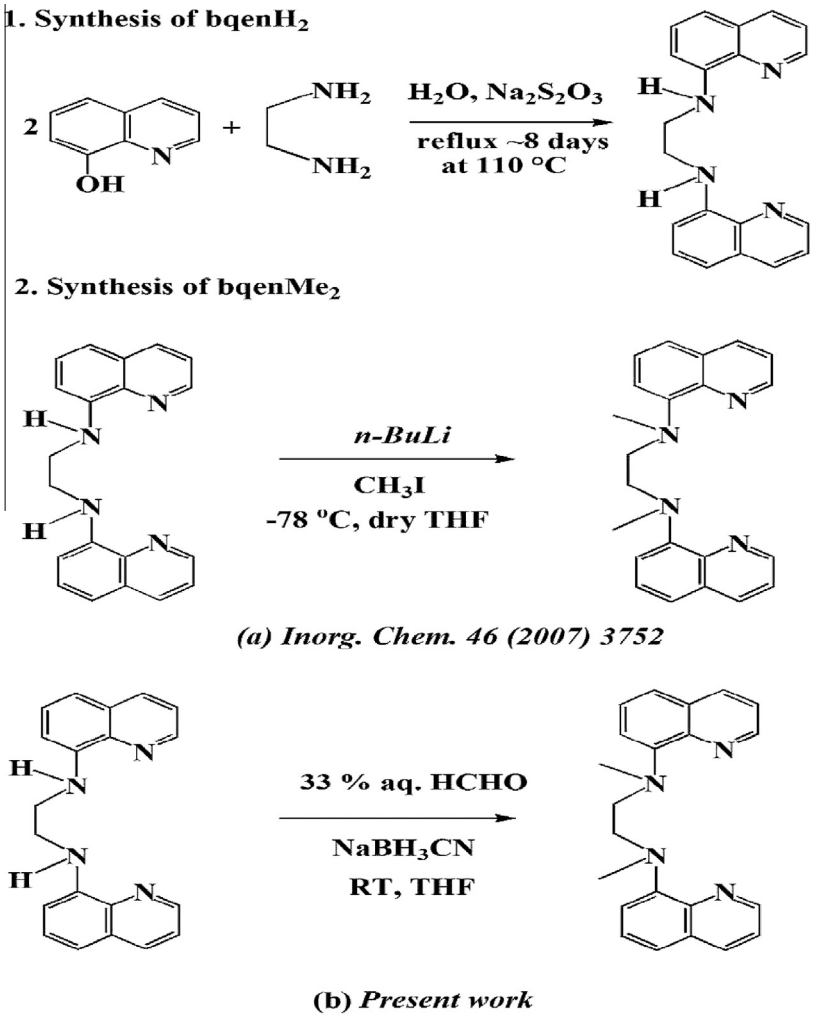

Scheme 2. Synthetic method used for the preparation of $bqenH_2$ and $bqenMe_2$.

2.2. Synthesis of ligands and compounds 1–6

2.2.1. Synthesis of N,N′-bis(8-quinolyl)ethane-1,2-diamine ($bqenH_2$)

The ligand $bqenH_2$ was prepared by following the literature procedure [33]. A mixture of 8-hydroxyquinoline (15.0 g, 103.3 mmol), ethylenediamine (3.1 g, 51.7 mmol), sodium metabisulphite (19.6 g, 103.3 mmol) and water (100 mL) was refluxed for about ~8 days at 110 °C. The reaction mixture was cooled at room temperature, then basified with aqueous sodium hydroxide solution (pH ~12) followed by extraction using dichloromethane (50 mL × 2). The solid formed after removal of dichloromethane was triturated with hot ethanol, filtered and then air dried. Yield of $bqenH_2$ (7.2 g, 44.0%). *Anal.* Calc. for $C_{20}H_{18}N_4$: C, 76.41; H, 5.77; N, 17.82. Found: C, 76.22; H, 5.62; N, 17.46%. IR (KBr, cm^{-1}): 3383 ν(NH); 1526 ν(C=N); ^{1}H NMR ($CDCl_3$, ppm): δ 8.69 (d, 2H, J = 2.2 Hz, 2-QnH), δ 8.06 (d, 2H, J = 2.2, 4-QnH), δ 7.37 (m, 4H, 3-QnH and 6-QnH), δ 7.07 (d, 2H, J = 8 Hz, 5-QnH), 6.77 (d, 2H, J = 4 Hz, 7-QnH), 6.42 (s, 2H, NH), 3.75 (s, 4H, NCH_2).

2.2.2. Synthesis of N,N′-dimethyl-N,N′-bis(8-quinolyl)ethane-1,2-diamine ($bqenMe_2$)

The ligand $bqenMe_2$ was prepared by a modification of the earlier procedure [33]. To a stirred THF solution (40 mL) of $bqenH_2$ (4.0 g, 12.7 mmol), about 21 mL of 37% aqueous formaldehyde (7.6 g, 254.5 mmol) was added. The solution slowly turned red after ~5 min. To this mixture solid sodium cyanoborohydride (1.6 g, 25.4 mmol) was added upon which the solution slowly turned to the original yellow color. The reaction mixture was then stirred for 24 h. The THF solvent was removed on a rotary evaporator and the yellow solid was filtered from the remaining aqueous solution. The compound was washed with cold ethanol for several times and dried under vacuum. The yellow solid was recrystallized from hot ethanol. Yield of $bqenMe_2$ (3.2 g, 74.0%). *Anal.* Calc. for $C_{22}H_{22}N_4$: C, 77.16; H, 6.48; N, 16.36. Found: C, 77.21; H, 6.64; N, 16.68%. IR (KBr, cm^{-1})1526 ν(C=N). ^{1}H NMR ($CDCl_3$, ppm): δ 8.76 (d, 2H, J = 6 Hz, 2-QnH,), δ 8.07(d, 2H, J = 6 Hz, 4-QnH), δ 7.36 (m, 6H, 3-, 5- and 6-QnH), δ 7.05(d, 2H, J = 6 Hz, 7-QnH), δ 3.96 (s, 4H, N-CH_2), δ 3.06 (s, 6H, NMe). ^{13}C NMR ($CDCl_3$, ppm): δ 149.3 (*ipso*), 147.3, 142.6 (*ipso*), 136.2, 129.6, 126.6, 120.73, 119.8, 115.5, 54.1 (N-CH_2), 41.3 (N-Me).

2.2.3. Synthesis of $[Ni(bqenH_2)(H_2O)_2](ClO_4)_2$ (**1**)

Green colored $Ni(ClO_4)_2{\cdot}6H_2O$ (2.2 g, 6.0 mmol) was dissolved in CH_3CN (5 mL). To this, was added a solution of $bqenH_2$ (1.9 g, 6.0 mmol) in CH_2Cl_2 (5 mL) in drop wise manner. Color of the reaction mixture was observed to change slowly from blue to violet. After 2 h diethyl ether (10 mL) was added to the reaction mixture to obtain violet colored crystalline solid which was isolated by filtration, washed with diethyl ether (10 mL) and finally air dried. Yield of **1** (3.0 g, 83.0%). *Anal.* Calc. for $C_{20}H_{22}N_4Cl_2O_{10}Ni$: C, 39.51; H, 3.65; N, 9.21. Found: C, 39.46; H, 3.33; N, 9.29%. IR (KBr, cm^{-1}): 3265 ν(NH); 1518 ν(C=N); 1093, 621 $\nu(ClO_4^{-1})$. λ_{max} (CH_3CN)/nm: 229, 302, 314, 528, 872 (ε/dm^3 mol^{-1} cm^{-1}) 58 500, 10 216, 8725, 8, 8.

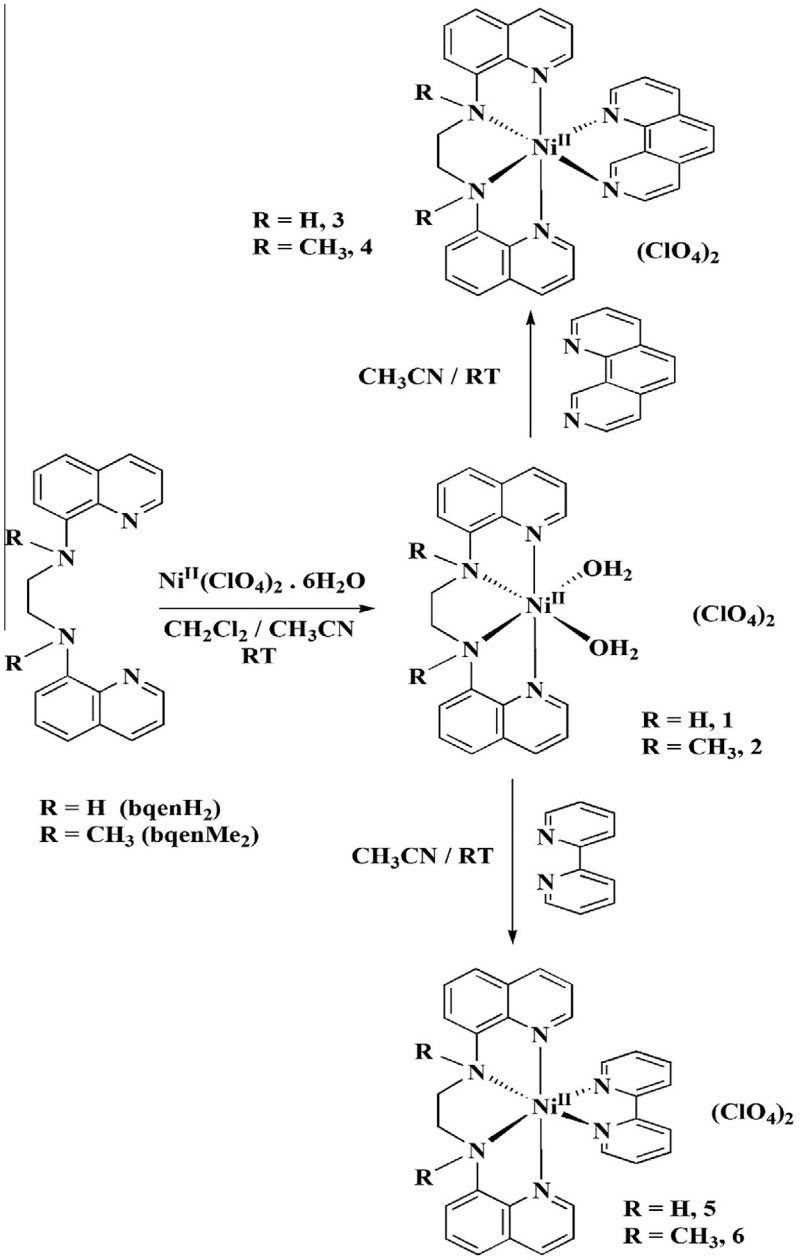

Scheme 3. Synthetic methodology used for the preparation of compounds **1**–**6**.

*2.2.4. Synthesis of [Ni(bqenMe$_2$)(H$_2$O)$_2$](ClO$_4$)$_2$ (**2**)*

The light pink colored compound was prepared by following the similar procedure as for compound **1** by taking bqenMe$_2$ (2.1 g, 6.0 mmol) instead of bqenH$_2$. Yield of **2** (3.1 g, 81.0%). *Anal.* Calc. for $C_{22}H_{26}N_4Cl_2O_{10}$ Ni: C, 41.54; H, 4.12; N, 8.81. Found: C, 41.16; H, 4.32; N, 8.65%. IR (KBr, cm^{-1}): 1518 ν(C=N); 1093, 621 ν(ClO_4^{-1}). λ_{max} (CH_3CN)/nm: 228, 302, 314, 528, 872 (ε/dm^3 mol^{-1} cm^{-1}): 57172, 11249, 9195, 9, 8.

*2.2.5. Synthesis of [Ni(bqenH$_2$)(phen)](ClO$_4$)$_2$ (**3**)*

Addition of CH_3CN (2 mL) solution of phen (0.20 g, 1.0 mmol) to the violet colored CH_3CN (3 mL) solution of **1** (0.61 g, 1.0 mmol) resulted in dark red colored solution. Slow diffusion of diethyl ether to this solution afforded red colored crystals after 4 days. Yield of **3** (0.6 g, 79.0%). *Anal.* Calc. for $C_{32}H_{26}N_6Cl_2O_8Ni$: C, 51.10; H, 3.48; N, 11.17. Found: C, 51.40; H, 3.71; N, 11.27%). IR (KBr, cm^{-1}): 3269 ν(NH); 1518 ν(C=N); 1093, 621 ν(ClO_4^{-1}). λ_{max} (CH_3CN)/nm: 227, 272, 294, 314, 589, 793 (ε/dm^3 mol^{-1} cm^{-1}) 65207, 30099, 15734, 7089, 21, 8.

*2.2.6. Synthesis of [Ni(bqenMe$_2$)(phen)](ClO$_4$)$_2$ CH$_3$CN (**4**)*

Similar procedure as mentioned for **3** was employed by reacting **2** (0.64 g, 1.0 mmol) in place of **1** to obtain violet colored crystals. Yield of **4** (0.62 g, 76.0%). *Anal.* Calc. for $C_{36}H_{33}N_7Cl_2O_8Ni$: C, 55.66; H, 4.05; N, 11.94. Found: C, 55.41; H, 4.17; N, 11.74%. IR (KBr, cm^{-1}): 1518 ν(C=N); 1093, 621 ν(ClO_4^{-1}). λ_{max} (CH_3CN)/nm: 225, 272, 296, 315, 501, 795 (ε/dm^3 mol^{-1} cm^{-1}) 67439, 23913, 31074, 6609, 11, 9.

*2.2.7. Synthesis of [Ni(bqenH$_2$)(bpy)](ClO$_4$)$_2$ (**5**)*

Reaction of bpy (0.16 g, 1.0 mmol) with compound **1** (0.61 g, 1.0 mmol) in CH_3CN resulted in dark reddish-brown colored solution. Slow diffusion of diethyl ether to this solution afforded dark reddish-brown colored crystalline compound. Yield of **5**

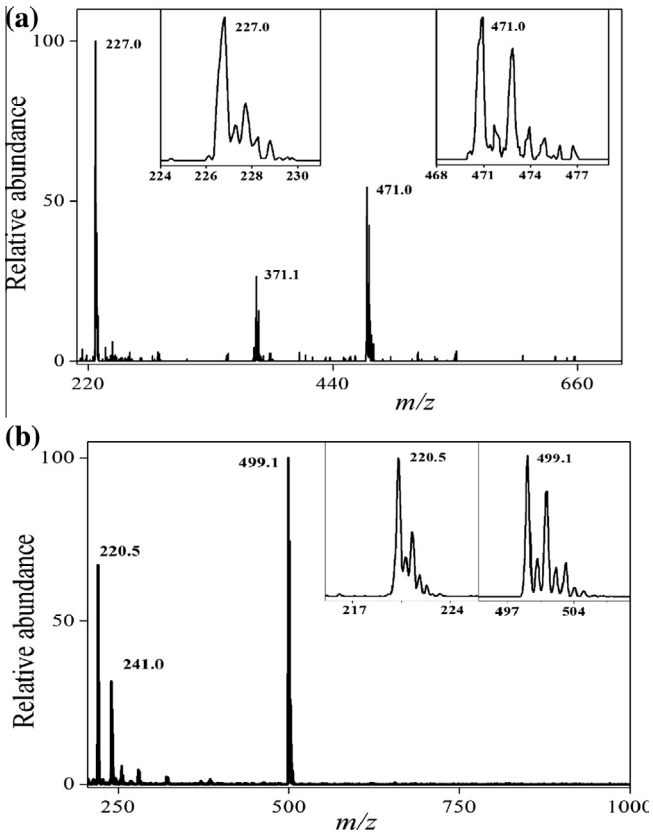

Fig. 2. ESI-MS spectrum of (a) **1** and (b) **2** measured in CH_3CN. Inset shows the isotope distribution patterns for the prominent peaks.

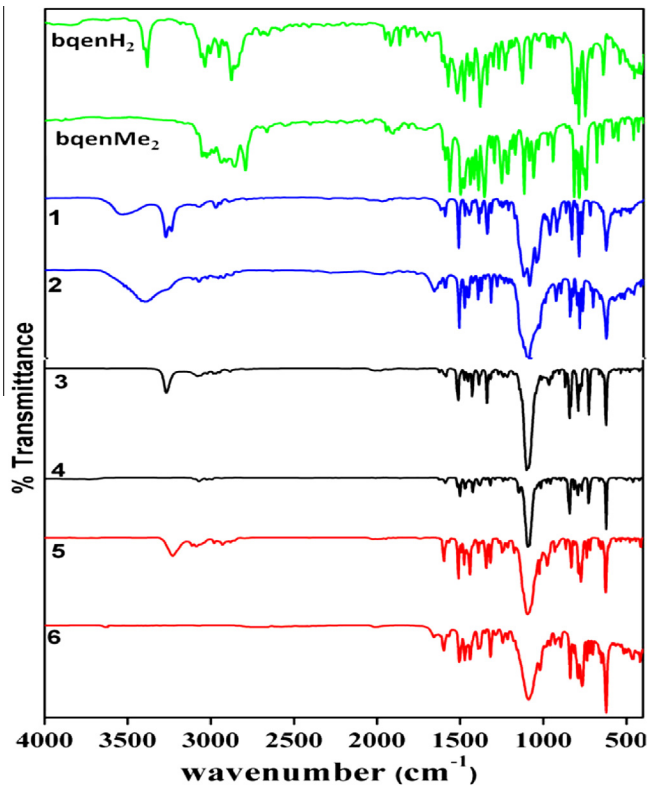

Fig. 3. Infrared spectra of ligands $bqenH_2$ and $bqenMe_2$ (green line), compounds **1**, **2** (blue line), **3**, **4** (black line) and **5**, **6** (red line). (For interpretation of the references to color in this figure legend, the reader is referred to the web version of this article.)

(0.7 g, 84.0%). *Anal.* Calc. for $C_{30}H_{26}N_6Cl_2O_8Ni$: C, 49.48; H, 3.60; N, 11.54. Found: C, 49.76; H, 3.35; N, 11.26%. IR (KBr, cm^{-1}): 3228 ν(NH); 1518 ν(C=N); 1093, 621 $\nu(ClO_4)^{-1}$. λ_{max} (CH_3CN)/nm: 230, 297, 308, 489, 793 (ε/dm^3 mol^{-1} cm^{-1}) 57596, 24834, 22673, 29, 9.

2.2.8. Synthesis of $[Ni(bqenMe_2)(bpy)](ClO_4)_2$ (**6**)

Similar procedure as mentioned for **5** was used in the preparation of **6**. Here the reaction of bpy with **2** (0.64 g, 1.0 mmol) resulted in the formation of reddish crystalline solid. Yield of **6** (0.6 g, 82.0%). Calc. for $C_{32}H_{30}N_6Cl_2O_8Ni$: C, 50.83; H, 4.00; N, 11.11%. Found: C, 50.74; H, 4.14; N, 11.38%. IR (KBr, cm^{-1}): 1518 ν(C=N); 1093, 621 $\nu(ClO_4)^{-1}$. λ_{max} (CH_3CN)/nm: 229, 283, 315, 528, 872 (ε/dm^3 mol^{-1} cm^{-1}) 56136, 19013, 7631, 10, 9.

3. Results and discussion

3.1. Description for the synthesis of ligands, complexes 1,2 and cis-ligand exchange to form **3–6**

The first iron(II) complex namely $[Fe(bqenMe_2)(CF_3SO_3)_2]$ of $bqenMe_2$ was reported by Britovsek et al. and shown to be an excellent catalyst for the oxidation of cyclohexane using H_2O_2 oxidant [33]. Nam and co-workers then demonstrated that $bqenMe_2$ complexes of manganese and iron such as $[Mn(bqenMe_2)(CF_3SO_3)_2]$ and $[Fe(bqenMe_2)(CF_3SO_3)_2]$ produce highly reactive intermediates that can oxidize alkanes and alcohols using peracetic acid [34,35]. The importance of $bqenMe_2$ ligand is thus clearly evidenced from these reports in biomimetic chemistry. For the ligand synthesis, the alkylation of R_2N–H is tedious and most challenging step which is normally carried out using an alkylating agent and strong base such as sodium hydride or *n*-butyllithium. However,

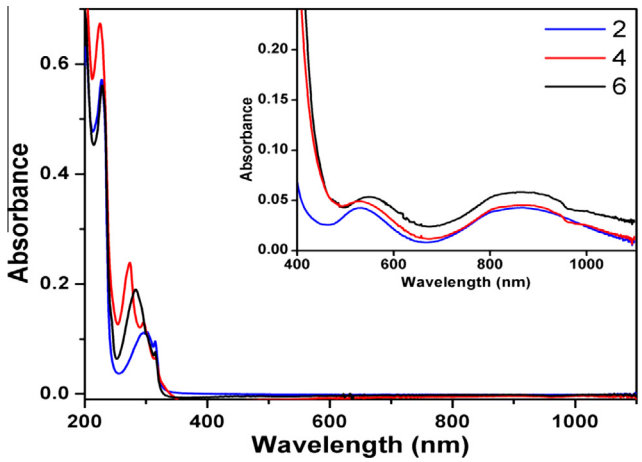

Fig. 4. Overlaid UV–Vis spectra of **2**, **4** and **6** (10^{-5} M) in CH_3CN. Inset show an expanded view of the region 400–1100 nm for *d*–*d* bands.

these reactions need special conditions such as dry solvents, inert atmospheres and low temperature (−78 °C). The synthesis of $bqenMe_2$ was earlier reported from the reaction of parent secondary amine $bqenH_2$, *n*-butyllithium and methyl iodide at −78 °C [33] (Scheme 2).

In this work, we have synthesized $bqenMe_2$ by a simple synthetic route that involves the reductive methylation of $bqenH_2$ using aqueous formaldehyde and sodium cyanoborohydride at room temperature (Scheme 2). The ligand $bqenH_2$ was prepared by following the reported procedure [33]. Both the ligands $bqenH_2$ and $bqenMe_2$ were characterized by ^1H and ^{13}C NMR spectroscopy

Table 1
UV–Vis data of compounds **1**–**6**.

Compound	$^3A_{2g} \rightarrow {}^3T_{1g}(F)$, nm ($\varepsilon$/dm^3 mol^{-1} cm^{-1})	$^3A_{2g} \rightarrow {}^3T_{2g}$, nm ($\varepsilon$/dm^3 mol^{-1} cm^{-1})
1	528 (8)	872 (9)
2	528 (9)	872 (8)
3	489 (21)	793 (8)
4	552 (11)	872 (9)
5	489 (29)	793 (9)
6	528 (10)	872 (12)

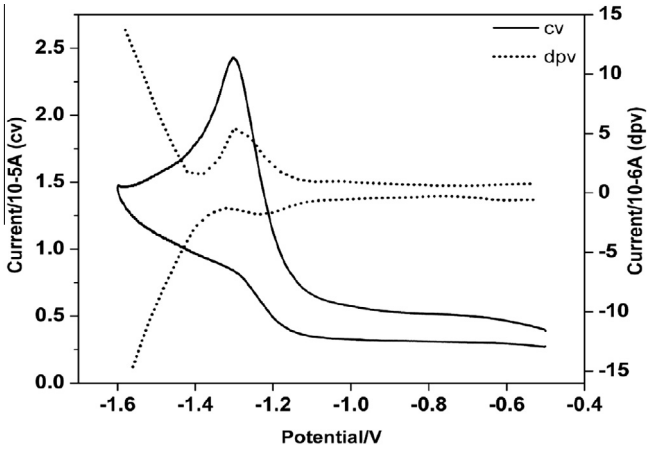

Fig. 5. CV (solid line) and DPV (dotted line) of **2** recorded at scan rate of 100 mV s^{-1} in DMSO containing 0.1 M of $TBAPF_6$ as supporting electrolyte.

(see Figs. S1–S4 in the supporting information). The reaction of $bqenH_2$ and $bqenMe_2$ with $Ni(ClO_4)_2{\cdot}6H_2O$ in CH_3CN afforded compounds **1** and **2** respectively in good yields. Our efforts to obtain the single crystals of compound **1** and **2** suitable for X-ray diffraction studies were not fruitful. Complex **1** was reacted with auxiliary bidentate N-donor ligands such as phen and bpy in CH_3CN resulting in the exchange of weakly coordinating solvent molecules (CH_3CN or H_2O) to obtain **3** and **5**. Under identical reaction conditions, the compounds **4** and **6** were prepared using **2** as a starting material. The single crystals of **3** and **4** were isolated on slow diffusion of diethyl ether into their solutions and directly used for X-ray data collection, however we were unable to grow the single crystals of **5** and **6**. The synthetic methodology adopted for the preparation of **1**–**6** is shown in Scheme 3.

3.2. ESI-Mass spectrometry

Compounds **1** and **2** were characterized by using ESI-Mass spectrometry in CH_3CN (see Fig. 2). The ESI-MS spectrum of **1**, shows prominent mass peaks at *m/z* 227.0 (calc. *m/z* 227.1) and 471.0 (calc. *m/z* 471.1) which are assigned to the $[Ni(bqenH_2)(CH_3CN)_2]^{2+}$ and $[Ni(bqenH_2)(ClO_4)]^{+}$ species respectively while the mass peak observed at *m/z* 371.1 (calc. *m/z* 371.0) is attributed to the $[Ni(bqenH)]^{+}$ species. On other hand, the ESI-MS spectrum of **2** exhibits prominent mass peaks at *m/z* 220.5 (calc. *m/z* 220.6), 241.0 (calc. *m/z* 241.1) and 499.1 (calc. *m/z* 499.1) which are assigned to the $[Ni(bqenMe_2)(CH_3CN)]^{2+}$, $[Ni(bqenMe_2)(CH_3CN)_2]^{2+}$ and $[Ni(bqenMe_2)(ClO_4)]^{2+}$ species respectively. Similarly, we have extended the ESI-MS spectrometry to the remaining complexes **3**–**6** (Fig. S5 in the supporting information).

The ESI-MS mass spectra of **3** and **4** show prominent mass peaks at m/z 276.0 (calc. *m/z* 276.1) and 290.0 (calc. *m/z* 290.1) which are assigned to the $[Ni(bqenH_2)(phen)]^{2+}$ and $[Ni(bqenMe_2)(phen)]^{2+}$ species respectively. For **5** and **6**, the mass peaks at 264.1 (calc. *m/z* 264.0) and 278.1 (calc. *m/z* 278.0) in the ESI-MS spectra are observed for $[Ni(bqenH_2)(bpy)]^{2+}$ and $[Ni(bqenMe_2)(bpy)]^{2+}$ species.

3.3. Infrared spectroscopy

The Infrared (IR) spectrum of $bqenMe_2$ shows absence of N-H vibration that is observed at ~3385 cm^{1-} for $bqenH_2$ (Fig. 3). This observation indicates that, the H atoms on two N atoms in $bqenH_2$ are replaced by the $-CH_3$ groups. The presence $-CH_3$ groups was further confirmed by the use of ^1H and ^{13}C NMR spectroscopy (Figs. S1–S4 in supplementary information). For compounds **1**, **3** and **5**, the N-H stretching vibrations occur at ~3265, 3269 and 3228 cm^{-1} respectively.

The N–H stretching vibrations in these three compounds are shifted to the lower frequencies as compared to that observed for the free ligand. This observation reveals that the ligand $bqenH_2$ is coordinated to the Ni(II) [36,37]. Further, no such bands were observed for compounds **2**, **4**, and **6** indicating the absence of N-H bonds in these compounds. Compounds **1** and **2** exhibit broad peaks at ~3547 cm^{-1} and ~3405 cm^{-1} respectively which are assigned to the O-H stretching vibrations of water. When **1** and **2** were dissolved in CH_3CN, the coordinated water molecules are exchanged with CH_3CN ligands [38]. The complete disappearance of -OH vibrations in **3**–**6** indicates the substitution of two H_2O molecules (which may be present as labile ligands) by bidentate phen and bpy in **3**–**6**. The presence of aromatic -C=N functionality is observed at ~1526 cm^{-1} for both the ligands while it is shifted to lower frequency of ~ 1518 cm^{-1} in all the compounds. This observation is not unusual as the two N donor atoms are coordinated to metal center [26,39,40]. The presence of perchlorate anions in **1**–**6** was revealed from the appearance of strong and medium absorption peaks at ~1093 and 621 cm^{-1} respectively [36,39].

3.4. UV–Vis spectroscopy

The electronic spectrum of nickel(II) ion in an octahedral environment is expected to show three *d*–*d* bands assignable for the $^3A_{2g} \rightarrow {}^3T_{2g}$, $^3A_{2g} \rightarrow {}^3T_{1g}(F)$ and $^3A_{2g} \rightarrow {}^3T_{1g}(P)$ transitions. The overlaid UV–Vis spectra of compounds **1**–**6** are shown in the Fig. 4 and Fig. S6 while the data for the intense *d*–*d* bands observed at different wavelengths in CH_3CN is summarized in the Table 1. The *d*–*d* band assigned to $^3A_{2g} \rightarrow {}^3T_{1g}(F)$ transition is observed in the region of 489–553 nm on the other hand the peak due to $^3A_{2g} \rightarrow {}^3T_{2g}$ transition is observed in the wavelength range 793–872 nm [41]. Both the bands are very weak in intensity and are observed only at higher concentrations of the compounds in CH_3CN. The tailing of a charge transfer band hinders the observation of third *d*–*d* band assigned to the $^3A_{2g} \rightarrow {}^3T_{1g}(P)$ transition in all six compounds [42].

The *d*–*d* absorption bands for **1** and **2** are similar in terms of their intensities and energies. Compounds **3** and **4** differ slightly in their absorption patterns from those of **5** and **6** which clearly suggests an influence of ligands (phen and bpy) on the crystal fields. The high-intensity bands observed in the UV region of 200–320 nm are assigned to the intra-ligand transitions. The band at ~272 nm in **3** and **4** is assigned to the π–π^* transition that arises from the coordination of the nickel to 1,10-phenanthroline [43]. The π–π^* transition due to bipyridine ligand is observed at 284 nm in compound 5 and at 296 nm in compound **6**. The bands in the region of 290–320 nm are assigned to the n–π^* transitions.

3.5. Cyclic and differential pulse voltammetry

Compounds **1**–**6** were characterized by using cyclic voltammetry (CV) and differential pulse voltammetry (DPV) to explore their

Table 2
Technical details of data acquisition and selected refinement results for **3** and **4**.

	Compound **3**	Compound **4**
Empirical formula	$C_{32}H_{26}Cl_2N_6\ NiO_8$	$C_{36}\ H_{33}Cl_2N_7NiO_8$
Formula weight	752.2	821.3
Crystal color	red	violet
Crystal system	orthorhombic	monoclinic
Space group	$P2_12_12_1$	$P2_1/c$
T (K)	100(2)	100(2)
Unit cell dimensions		
a (Å)	11.304(2)	18.0780(4)
b (Å)	15.972(3)	11.3105(2)
c (Å)	17.680(3)	17.2253(3)
α (°)	90.00	90.00
β (°)	90.00	100.37
γ (°)	90.00	90.00
V (Å^3)	3192.3(10)	3464.58(12)
Z	4	4
Radiation type (Mo Kα) (Å)	0.71073	0.71073
Crystal size (mm)	0.30 × 0.20 × 0.10	0.20 × 0.20 × 0.10
Diffractometer	Bruker APEX-II CCD	Bruker APEX-II CCD
Absorption correction	None	None
Number of measured reflections	9790	9803
D_{calc} (g/cm^3)	1.565	1.575
Absorption coefficient (mm^{-1})	0.838	0.780
F(000)	1544	1696
θ range for data collection	2.14–28.37	2.40–28.31
Flack parameter	0.00	–
Limiting indices	$-15 \leqslant h \leqslant 15$, $-21 \leqslant k \leqslant 21$, $-23 \leqslant l \leqslant 23$	$-22 \leqslant h \leqslant 22$, $-13 \leqslant k \leqslant 13$, $-21 \leqslant l \leqslant 21$
Refinement method	SHELXS-97	SHELXS-97
Data/restraints/parameter	7919/0/442	6817/0/490
Final R indices[I > 2σ(I)]	R_1 = 0.0233, wR_2 = 0.0592	R_1 = 0.0299, wR_2 = 0.1182
R indices (all data)	R_1 = 0.0250, wR_2 = 0.0604	R_1 = 0.0341, wR_2 = 0.1239
Goodness of fit (GOF) on F^2	0.966	1.071

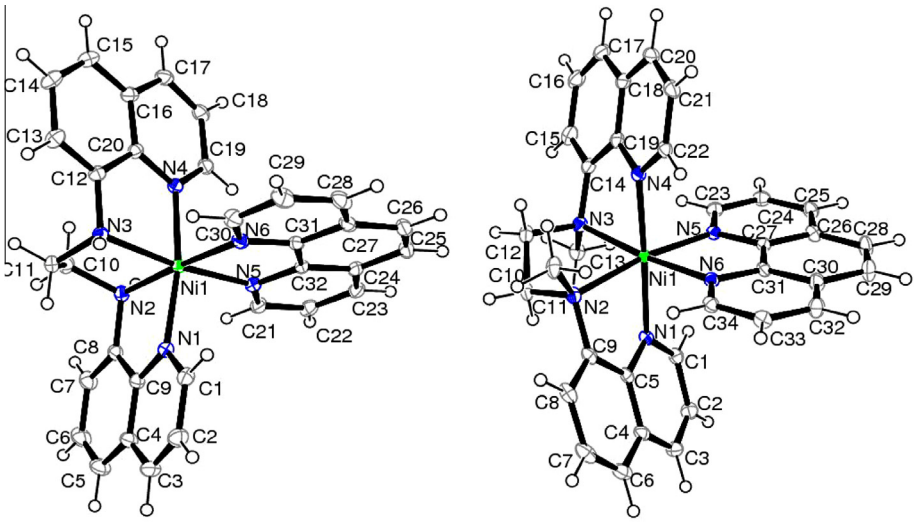

Fig. 6. The crystal structure of $[Ni(bqenH_2)]^{2+}$ cation in **3** (left) and $[Ni(bqenMe_2)]^{2+}$ cation in **4** (right) showing the atom labeling scheme. Displacement ellipsoids are drawn at 50% probability level except for the H atoms, which are shown as circles of arbitrary radius (top). The perchlorate anions are omitted for clarity.

electrochemical properties. The CV and DPV plots of compound **2** are depicted in Fig. 5. Compounds **1** and **2** exhibit a quasi-reversible cathodic and anodic waves which can be attributed for the reduction of Ni(II)/Ni(I) and N(I)/Ni(II) couples, for which the $E_{1/2}$ value is centered at ~−1.3 volts (V) [44–48]. The anodic potential wave for compounds **1**–**6**, is poorly resolved in CV plots but same is distinctly visible in the DPV plots (see Fig. S7 in the supporting information). The CV and DPV plots of compounds **3** and **4** are similar to those of compounds **1** and **2** with $E_{1/2}$ value centered at ~−1.45 V. Further, the $E_{1/2}$ value for Ni(II)/Ni(I) couple in compounds **5** and **6** is nearly the same as that observed in **1** and **2**. A poorly resolved anodic peak at ~0.13 V (data not shown) for the oxidation of Ni(II) to Ni(III) species and the corresponding cathodic peak for the reduction of Ni(III) to Ni(II) species was also observed. The cyclic voltammograms recorded at different scan rates were identical and the peak currents increased proportionally with the increase in scan rates (see Fig. S8 for **1** in the supporting information). The CV and DPV plots of $bqenH_2$ as well as $bqenMe_2$ show no oxidation–reduction peaks in the measured potential range and thus suggest that the both ligands are electrochemically inactive under the experimental conditions (see Fig. S9 in the supporting information for CV and DPV of $bqenMe_2$). Hence, the observed peaks in the cyclic voltammograms of **1** and **2**

Table 3
Selected bond lengths (Å) and angles (°) for **3** and **4**.

Compound ***3***			
Bond length (Å)			
Ni1–N5	2.085(1)	Ni1–N4	2.097(1)
Ni1–N6	2.086(1)	Ni1–N2	2.104(1)
Ni1–N1	2.092(1)	Ni1–N3	2.126(1)
Bond angle (°)			
N5–Ni1–N6	80.10(5)	N1–Ni1–N2	80.69(5)
N5–Ni1–N1	93.50(5)	N4–Ni1–N2	90.41(5)
N6–Ni1–N1	97.34(5)	N5–Ni1–N3	172.67(5)
N5–Ni1–N4	97.34(5)	N6–Ni1–N3	98.30(5)
N6–Ni1–N4	91.76(5)	N1–Ni1–N3	93.80(5)
N1–Ni1–N4	169.89(5)	N4–Ni1–N3	80.48(5)
N5–Ni1–N2	97.41(5)	N2–Ni1–N3	84.43(5)
N6–Ni1–N2	176.76(5)		
Compound 4			
Bond length (Å)			
Ni1–N4	2.067(1)	Ni1–N5	2.116(2)
Ni1–N1	2.079(1)	Ni1–N3	2.162(2)
Ni1–N6	2.111(2)	Ni1–N2	2.182(2)
Bond angle (°)			
N4–Ni1–N1	177.84(6)	N6–Ni1–N3	173.76(6)
N4–Ni1–N6	94.98(6)	N5–Ni1–N3	99.22(6)
N1–Ni1–N6	86.41(6)	N4–Ni1–N2	100.11(6)
N4–Ni1–N5	88.14(6)	N1–Ni1–N2	78.06(6)
N1–Ni1–N5	93.74(6)	N6–Ni1–N2	97.54(6)
N6–Ni1–N5	79.42(6)	N5–Ni1–N2	171.47(6)
N4–Ni1–N3	78.85(6)	N3–Ni1–N2	84.63(6)
N1–Ni1–N3	99.78(6)		

Note: The values in the parentheses indicate estimated standard deviations.

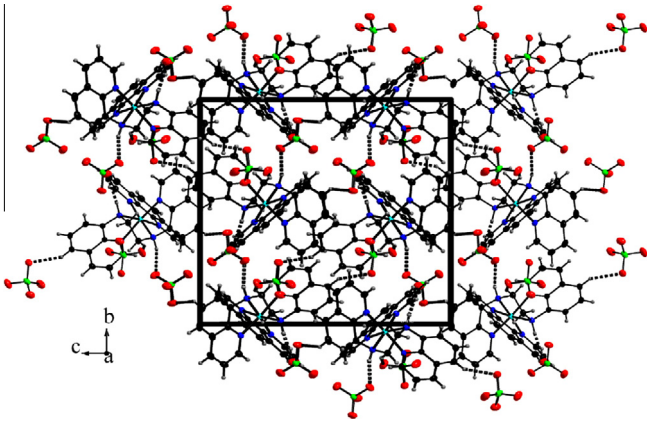

Fig. 7. A view of the packing diagram of **3** along the *a*-axis. N–H···O and C–H···O hydrogen bonds are shown as dashed lines. Color code: C, black; H, medium grey; N, blue; O, red; Cl, green and Ni, sky blue. (For interpretation of the references to color in this figure legend, the reader is referred to the web version of this article.)

are solely assigned to the quasi-reversible redox process of Ni(II)/Ni(I) couple.

3.6. Description for the crystal structures of compounds 3 and 4

All six compounds **1**–**6** were obtained as crystalline solids, however we were able to grow the single crystals of compounds **3** and **4** which were characterized by X-ray crystallography. Single crystals suitable for structure determination were obtained by slow diffusion of diethyl ether into the CH_3CN solutions of **3** and **4**. The technical details of data acquisition and selected refinement results for **3** and **4** are given in Table 2. Compound **3** crystallizes in the non-centrosymmetric orthorhombic space group $P2_12_12_1$, while **4** crystallizes in the centrosymmetric monoclinic space group $P2_1/c$. In both compounds all atoms are located in their general positions. The crystal structure of **3** and **4** contains a central nickel(II), a unique N4 ligand ($bqenH_2$ in **3** and $bqenMe_2$ in **4**), one phen ligand and two crystallographically independent perchlorate ions (Fig. 6). Interestingly, the compound **4** has an additional uncoordinated CH_3CN molecule in its crystal lattice (see Fig. S10) and this unique feature is absent in compound **3**.

The perchlorate ions behaves as charge balancing counter anions. The quinolyl nitrogen atoms N1 and N4 are *trans* to each other while the amine nitrogen atoms N2 and N3 occupy the adjacent positions. The two methyl groups, one on N2 and the other on N3 atoms of $bqenMe_2$ in **4** are located *anti* to each other unlike the *syn* H atoms on N2 and N3 atoms of $bqenH_2$ in **3**. The auxiliary ligand phen occupy the positions of two labile *cis*-ligands (CH_3CN or H_2O) through N5 and N6 atoms thereby completing the NiN6 octahedron (see Fig. S10). All the Ni–N bond distances and N–Ni–N bond angles are in normal range (Table 3) and are in good agreement with literature reports [31,42,49–53].

In both the complexes the N–Ni–N *trans* and *cis* angles deviates from 180° and 90° respectively suggesting the distortion of octahedral geometry. The *trans* angles in **3** ranges from 169.89(5)° to 176.76(5)° and in **4** it ranges from 171.47(6)° to 177.84(6)°. Whereas the *cis* angles vary between 80.10(5) to 98.30(5) in **3** and 79.42(6) to 100.11(6) in **4**. The Ni-N bond distances lies from 2.085(1) to 2.126(1) in complex **3** and 2.067(1) to 2.182(2) in complex **4**. Further, the electronegative atoms (N and O as well as C) in these compounds are involved in the intermolecular hydrogen bonding (N–H···O, C–H···O in **3** and only C–H···O in **4**) forming a supramolecular three-dimensional networks as shown in Fig. 7 and Fig. 8. The N–H···O and C–H···O hydrogen bonds are shorter than the sum of their Van der Waals radii revealing the strength of these H-bonds in stabilizing overall crystal structures of **3** and **4** (Table 4).

In the crystal structure of **4**, which lacks the N–H bonds, only C–H bonds of $bqenMe_2$ are involved in the C–H···O interactions with neighboring O atoms of perchlorate anions while structure of **3** is stabilized by the strong N–H···O and C–H···O interactions. Fig. S11 and S12 displays a symmetric organization of the octahedral units in **3** and **4** respectively.

3.7. Catalytic hydroxylation of alkanes by *1*–*6*

Compounds **1**–**6** were tested for the efficacy of catalytic oxidations of hydrocarbons such as cumene, ethylbenzene, and cyclohexane using *m*-CPBA as an oxidant in CH_3CN at 25 °C under N_2 atmosphere. The hydroxylated products of alkanes were analyzed and quantified by gas chromatography (GC) using authentic samples and decane as an internal standard. Compounds **1**–**2** efficiently catalyzed the hydroxylation of C-H bonds in alkanes used in this study, however no organic products were obtained in the catalytic reactions when compounds **3**–**6** were used (Table 5, Scheme 4). There is no surprise in this observation as in the compounds **3**–**6**, the Ni(II) center is coordinatively saturated with the strongly bonded six donor N atoms (four of quinoline moiety and two each of phenanthroline or bipyridine) which has resulted in the poor oxidizing power of **3**–**6**. We propose a compounds **1** and **2** have an octahedral geometry with two H_2O molecules occupying the *cis*-positions. However, in the CH_3CN solution, the two H_2O molecules are exchanged rendering the two CH_3CN molecules at *cis* positions. The *cis*-ligands are thus labile and make nickel(II) center more susceptible for the oxidation by *m*-CPBA oxidant.

A comparative reactivity of **1** and **2**, reveals that compound **2** gives higher yield of hydroxylated products (Table 5). The high yield of alcohol and ketone using compound **2**, can be attributed to the differing nature of ligand in **1** and **2**. In compound **1**, the $bqenH_2$ has a secondary amine tail (R_2NH) on the other had in **2** the $bqenMe_2$ has all alkylated N atoms making it tertiary amine.

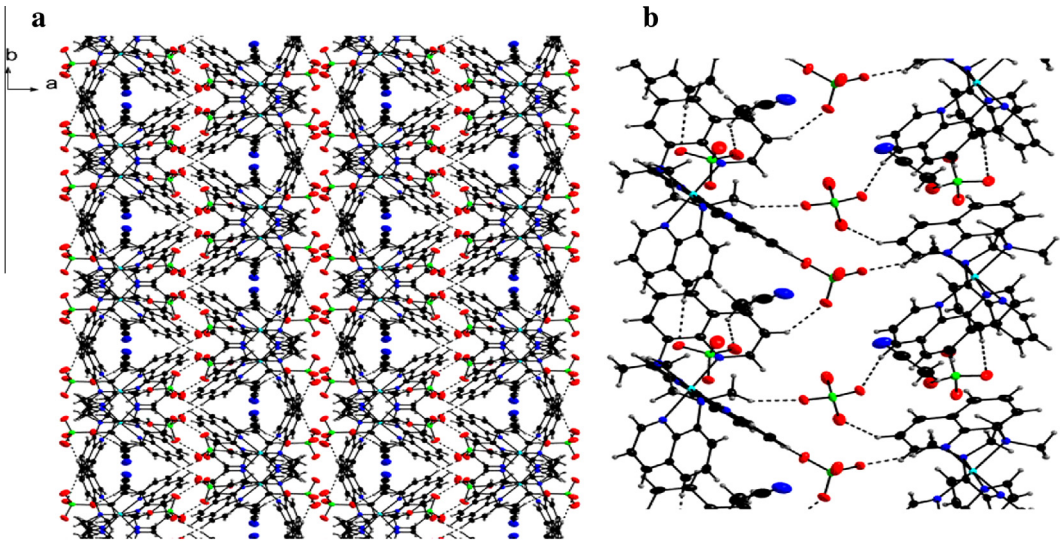

Fig. 8. (a) Helical style symmetric organization of $[Ni(bqen)(phen)]^{2+}$ cations and ClO_4^- anions with the pockets occupied by CH_3CN molecules in **4** along the *c*-axis. (b) Hydrogen bonding diagram showing C–H···O interactions between cation $[Ni(bqen)(phen)]^{2+}$ and ClO_4^- anion in **4**. Color code: C, black; H, medium grey; N, blue; O, red; Cl, green and Ni, sky blue. (For interpretation of the references to color in this figure legend, the reader is referred to the web version of this article.)

Table 4
Hydrogen bonding parameters (Å, °) for **3** and **4**.

Compound ***3***				
D–H···A	D–H/Å	H···A/Å	D···A/Å	D–H···A/°
C(15)–H(15)···O7[a]	0.95(2)	2.397(1)	3.203(2)	142.45(11)
C(6)–H(6)···O3[b]	0.951(2)	2.418(1)	3.255(2)	146.72(13)
C(10)–H(10A)···O6	0.99(2)	2.307(1)	3.197(2)	148.94(10)
N(2)–H(31)···O4	0.93(1)	2.087(1)	2.990(2)	163.57(9)
N(3)–H(32)···O1[c]	0.93(1)	2.201(1)	3.126(2)	172.90(9)
Compound ***4***				
C(10)–H(10C)···O8[a]	0.981(2)	2.418(2)	3.321(3)	152.97(12)
C(32)–H(32)···O5[b]	0.951(2)	2.422(2)	3.288(2)	151.39(12)
C(6)–H(6)···O3[c]	0.950(2)	2.486(2)	3.432(3)	173.99(13)
C(36)–H(36B)···O2	0.979(3)	2.439(2)	3.198(3)	134.08(16)
C21(3)–H(21)···O7[d]	0.950(2)	2.306(2)	3.082(3)	138.41(13)

[a] –0.5 + *x*, 0.5 – *y*, 1 – *z*, [b] –0.5 + *x*, 0.5 – *y*, 2 – *z*, [c] 1 – *x*, 0.5 + *y*, 1.5 – *z* for **3**
[a] *x*, *y*, 1 + *z*, [b] –*x*, – 0.5 + *y*, 0.5 – *z*, [c] *x*, 0.5 – *y*, 0.5 + *z* [d] –*x*, 0.5 + *y*, 0.5 – *z* for **4**
Note: The values in the parentheses indicate estimated standard deviations.

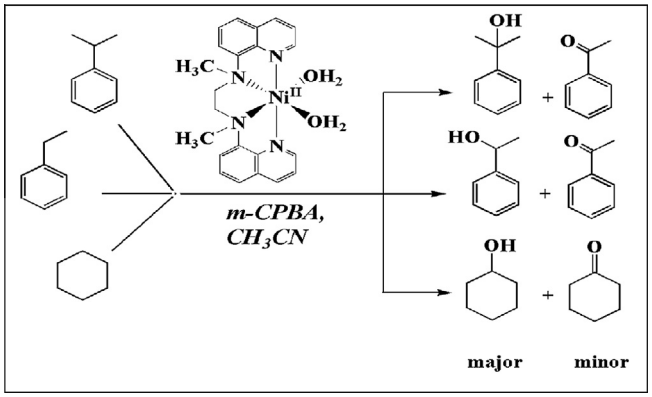

Scheme 4. Alkane hydroxylation by $[Ni(bqenMe_2)(H_2O)_2]^{2+}$ **2** in CH_3CN using *m*-CPBA oxidant.

In biomimetic non-heme oxidation chemistry, the $bqenMe_2$ complexes of iron(II) and manganese(II) have been used instead of $bqenH_2$ [33–35]. The oxidation of cyclam ligand which has four R_2NH groups, is reported in Ni(II)-cyclam complexes using H_2O_2 as oxidant [54]. It is likely that in **1**, the $bqenH_2$ which has secondary amine functionality can undergo partial oxidation thus reflecting on the observed low yields of organic products compared to **2** (Table 5). In the oxidation of cumene, 2-phenylpropan-2-ol was obtained in high yield while acetophenone and 2-methylstyrene were obtained as minor products. Use of ethylbenzene instead of cumene as a substrate, resulted in high yield of 1-phenylethanol along with minor products acetophenone and styrene.

Table 5
Organic product analysis using GC in the alkane hydroxylation by **1**–**6**[a].

Catalyst	Substrate	Alcohol[c]	(TON)[b] (A)	Ketone	(TON)[b] (K)	A/K
1	Cumene	2-Phenylpropan-2-ol	105	Acetophenone	23	4.6
	Ethylbenzene	1-Phenylethanol	121	Acetophenone	25	4.8
	Cyclohexane	Cyclohexanol	116	Cyclohexanone	23	5.0
2	Cumene	2-Phenylpropan-2-ol	361	Acetophenone	42	8.6
	Ethylbenzene	1-Phenylethanol	390	Acetophenone	38	10.3
	Cyclohexane	Cyclohexanol	410	Cyclohexanol	50	8.2
3–**6**	Cumene	2-Phenylpropan-2-ol	NIL	Acetophenone	NIL	NIL
	Ethylbenzene	1-Phenylethanol		Acetophenone		
	Cyclohexane	Cyclohexanol		Cyclohexanol		

Note:
[a] Reaction conditions: $[Ni^{2+}]$ = 0.5 mM; [m-CPBA] = 0.5 M, [substrate] = 1 M in CH_3CN at 25 °C for 90 min under N_2.
[b] Turnover number [(moles of product)/(moles of catalyst)] determined by GC.
[c] Small amounts of desaturated products in the case of cumene and ethylbenzene while the small amount of ε-caprolactone in case of cyclohexanone were observed.

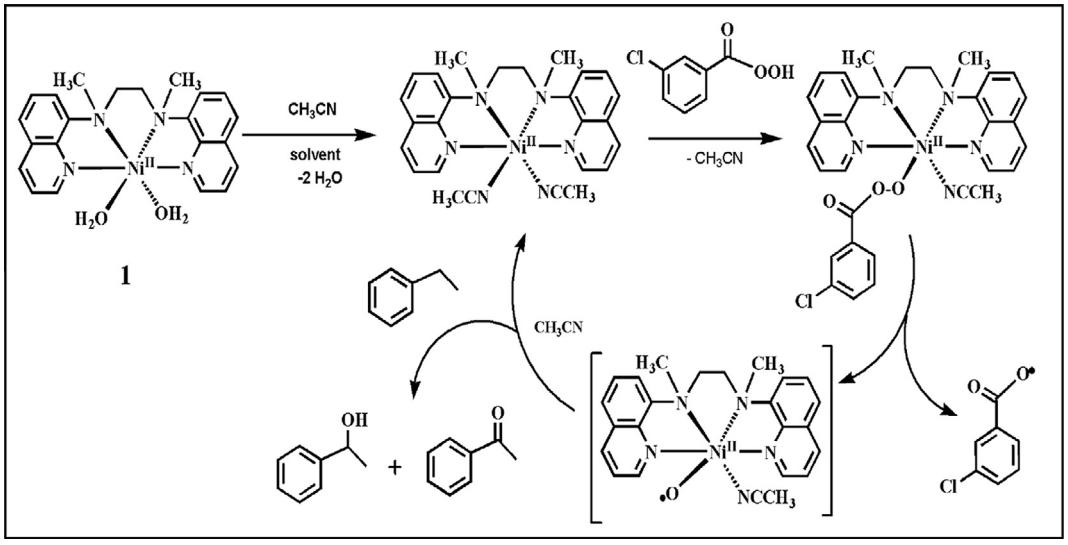

Scheme 5. Proposed mechanism for the alkane hydroxylation by $[Ni(bqenMe_2)(H_2O)_2]^{2+}$ using *m*-CPBA oxidant.

Cyclohexane was selectively oxidized to cyclohexanol with low yields of cyclohexanone and caprolactam. A mechanism for the C–H activation of alkanes to hydroxylated products is proposed under the similar lines as reported by others [17,21–25]. As shown in Scheme 5, the $[Ni(II)(bqen)(CH_3CN)(m\text{-CPBA})]^+$ adduct results in the generation of reactive intermediates $[Ni^{II}\text{-}O\cdot(bqen)(CH_3CN)]^+$ and *m*-chlorobenzoic acid radical via homolytic cleavage of O–O bond.

We propose that an intermediate $[Ni^{II}\text{-}O\cdot(bqen)(CH_3CN)]^+$ is responsible for the hydroxylation of alkanes giving us alcohols as the major products. Efforts are underway to investigate the alkane hydroxylation reactions using other transition metal compounds of tetradendate tripodal ligands.

4. Conclusions

In this paper, we have reported the synthesis and characterization of six new Ni(II) octahedral complexes **1**–**6** containing the tetradentate tripodal ligands $bqenH_2$ and $bqenMe_2$. Further, when **1** and **2** were reacted with the auxiliary ligands such as phen and bpy we obtained compounds **3**–**6** by a simple replacement of labile CH_3CN molecules. Compounds **3** and **4** were structurally characterized. CV and DPV experiments revealed the Ni(II)/Ni(III) and Ni(II)/Ni(I) quasi-reversible processes in compounds **1**–**6** against SCE in DMSO. All the compounds **1**–**6** were tested in the hydroxylation of alkanes using *m*-CPBA oxidant under catalytic conditions. Only **1** and **2** were found to be highly selective in hydroxylating the C-H bonds of alkanes giving alcohols as major products. Interestingly, compound **2** afforded us high TON (turn over number) of alcohol and ketone compared to **1**. The observation of high A/K (alkohol/ketone) ratio in the alkane hydroxylation by **1** and **2** thus make these compounds as highly efficient catalysts for alcohol production. The four compounds **3**–**6** are coordinatively saturated with six donor N atoms making them poor catalysts for alkane oxidation.

Acknowledgment

SND thank University Grant Commission (UGC), New Delhi (F.No.37-576/2009 (SR) and Department of Science and Technology (DST), New Delhi (SR/FT/CS-006/2010) for the financial support. DDN thank UGC for Junior Research Fellowship (UGC-BSR-JRF). The Department of Chemistry, Goa University, receives the grants from UGC-SAP and DST-FIST programs of UGC and DST, New Delhi. SND thank Prof. Wonwoo Nam, Ewha Womans University and Prof. Jaeheung Cho, Daegu Gyeongbuk Institute of Science & Technology, for their help in providing us crystal data. Authors thank Prof. B. R. Srinivasan, Goa University for helpful discussion.

Appendix A. Supplementary material

CCDC 948509 and 1019725 contains the supplementary crystallographic data for **3** and **4**. These data can be obtained free of charge from The Cambridge Crystallographic Data Centre via www.ccdc.cam.ac.uk/data_request/cif. Supplementary data associated with this article can be found, in the online version, at http://dx.doi.org/10.1016/j.ica.2015.01.009. These data include MOL files and InChiKeys of the most important compounds described in this article.

References

[1] M. Zhang, Z.-Y. Gu, M. Bosch, Z. Perry, H.-C. Zhou, Coord. Chem. Rev. (2015) (doi: 10.1016/j.ccr.2014.05.031) (in press).
[2] S.C. Sawant, X. Wu, J. Cho, K.-B. Cho, S.H. Kim, M.S. Seo, Y.-M. Lee, M. Kubo, T. Ogura, S. Shaik, W. Nam, Angew. Chem., Int. Ed. 49 (2010) 8190.
[3] N. Saravanan, M. Palaniandavar, Inorg. Chim. Acta 385 (2012) 100.
[4] S. Yu, C.-X. Miao, D. Wang, S. Wang, C. Xia, W. Sun, J. Mol. Catal. A 353–354 (2012) 185.
[5] X. Wu, M.S. Seo, K.M. Davis, Y.-M. Lee, J. Chen, K.-B. Cho, Y.N. Pushkar, W. Nam, J. Am. Chem. Soc. 133 (2011) 20088.
[6] J. Annaraj, S. Kim, M.S. Seo, Y.-M. Lee, Y. Kim, Inorg. Chim. Acta 362 (2009) 1031.
[7] G.J.P. Britovsek, J. England, A.J.P. White, Inorg. Chem. 44 (2005) 8125.
[8] Y. He, C.R. Goldsmith, Chem. Commun. 48 (2012) 10532.
[9] S.N. Dhuri, M.S. Seo, Y.-M. Lee, H. Hirao, Y. Wang, W. Nam, S. Shaik, Angew. Chem., Int. Ed. 47 (2008) 3356.
[10] Y.-M. Lee, S.N. Dhuri, S.C. Sawant, J. Cho, M. Kubo, T. Ogura, S. Fukuzumi, W. Nam, Angew. Chem., Int. Ed. 48 (2009) 1803.
[11] J. Kaizer, E.J. Klinker, N.Y. Oh, J.-U. Rohde, W.J. Song, A. Stubna, J. Kim, E. Munck, W. Nam, L. Que Jr., J. Am. Chem. Soc. 126 (2004) 472.
[12] D. Maiti, H.R. Lucas, A.A.N. Sarjeant, K.D. Karlin, J. Am. Chem. Soc. 129 (2007) 6998.
[13] D. Maiti, H.C. Fry, J.S. Woertink, M.A. Vance, E.I. Solomon, K.D. Karlin, J. Am. Chem. Soc. 129 (2007) 264.
[14] T. Tano, Y. Okubo, A. Kunishita, M. Kubo, H. Sugimoto, N. Fujieda, T. Ogura, Inorg. Chem. 52 (2013) 10431.
[15] J. Cho, R. Sarangi, H.Y. Kang, J.Y. Lee, M. Kubo, T. Ogura, E.I. Solomon, W. Nam, J. Am. Chem Soc. 132 (2010) 16977. and references cited therein.
[16] T. Nagataki, Y. Tachi, S. Itoh, Chem. Commun. (2006) 4016
[17] J. Cho, R. Sarangi, J. Annaraj, S.Y. Kim, M. Kubo, T. Ogura, E.I. Solomon, W. Nam, Nat. Chem. 1 (2009) 568.

[18] M.T. Kieber-Emmons, J. Annaraj, M.S. Seo, K.M. Van Heuvelen, T. Tosha, T. Kitagawa, T.C. Brunold, W. Nam, C.G. Riordan, J. Am. Chem. Soc. 128 (2006) 14230.
[19] J. Cho, H.Y. Kang, L.V. Liu, R. Sarangi, E.I. Solomon, W. Nam, Chem. Sci. 4 (2013) 1502.
[20] M. Balamurgan, R. Mayilmurugan, E. Suresh, M. Palaniandavar, Dalton Trans. 40 (2011) 9413.
[21] S. Hikichi, K. Hanaue, T. Fujimura, H. Okuda, J. Nakazawa, Y. Ohzu, C. Kobayashi, M. Akita, Dalton Trans. 42 (2013) 3346.
[22] S. Hikichi, H. Okuda, Y. Ohzu, M. Akita, Angew. Chem., Int. Ed. 48 (2009) 188.
[23] J. Nakazawa, S. Terada, M. Yamada, S. Hikichi, J. Am. Chem. Soc. 135 (2013) 6010.
[24] T. Nagataki, K. Ishii, Y. Tachi, S. Itoh, Dalton Trans. (2007) 1120
[25] E. Ramachandran, D.S. Raja, J.L. Mike, T.R. Wagner, M. Zeller, K. Natarajan, RSC Adv. 2 (2012) 8515.
[26] E.N. Nfor, S.N. Esemu, G.A. Ayimele, E.A. Eno, G.E. Iniama, O.E. Offiong, Bull. Chem. Soc. Ethiop. 25 (2011) 361.
[27] L.R. Gomes, J.N. Low, M.A.A. Rocha, L.M.N.B.F. Santos, B. Schröder, P. Brandão, C. Matos, J. Neves, J. Mol. Struct. 990 (2011) 86.
[28] L. Zhu, D.-M. Kong, X.-Z. Li, G.-Y. Wang, J. Wang, Y.-W. Jin, Polyhedron 29 (2010) 574.
[29] C.N. Sudhamani, H.S. Bhojya Naik, T.R. Ravikumar Naik, M.C. Prabhakara, Spectrochim. Acta, Part. A 72 (2009) 643.
[30] A.E.-M.M. Ramadan, J. Mol. Struct. 1015 (2012) 56.
[31] K.C. Skyrianou, V. Psycharis, C.P. Raptopoulou, D.P. Kessissoglou, G. Psomas, J. Inorg. Biochem. 105 (2011) 63.
[32] G.M. Sheldrick, SHELXTL/PC. Version 6.12 for Windows XP, Bruker AXS Inc., Madison, WI, USA (2001).
[33] J. England, G.J.P. Britosvek, N. Rabadla, A.J.P. White, Inorg. Chem. 46 (2007) 3752.
[34] K. Nehru, S.J. Kim, I.Y. Kim, M.S. Seo, Y. Kim, S.-J. Kim, J. Kim, W. Nam, Chem. Commun. (2007) 4623
[35] J. Yoon, S.A. Wilson, Y.K. Jang, M.S. Seo, K. Nehru, B. Hedman, K.O. Hodgson, E. Bill, E.I. Solomon, W. Nam, Angew. Chem., Int. Ed. 48 (2009) 1257.
[36] K. Nakamoto, Infrared and Raman Spectra of Inorganic and Coordination Compounds, sixth ed., John Wiley & Sons, 2008.
[37] B.V. Kumar, H.S. Bhojya Naik, D. Girija, N. Sharath, S.M. Pradeepa, H.J. Hoskeri, M.C. Prabhakara, Spectrochim. Acta, Part. A 94 (2012) 192.
[38] A.E. Wickenden, R.A. Krause, Inorg. Chem. 4 (1965) 404.
[39] P. Bhowmik, M.G.B. Drew, S. Chattopadhyay, Inorg. Chim. Acta 366 (2011) 62.
[40] R. Pastorek, Z. Trávníček, P. Štarha, Inorg. Chim. Acta 373 (2011) 286.
[41] R. Ivaniková, R. Boča, L. Dlháň, H. Fuess, A. Mašlejová, V. Mrázova, I. Svoboda, J. Titiš, Polyhedron 25 (2006) 3261.
[42] M.A. Ali, A.H. Mirza, F.H. Bujang, M.H.S.A. Hamid, P.V. Bernhardt, Polyhedron 25 (2006) 3245.
[43] A.I. El-Said, A.S.A. Zidan, M.S. El-Meligy, A.A.M. Aly, O.F. Mohammed, Trans. Met. Chem. 26 (2001) 13.
[44] K.-Y. Choi, S.N. Choi, I.-H. Suh, Polyhedron 17 (1998) 1415.
[45] H. Temel, S. İlhan, M. Aslanoğlu, A. Kılıçl, E. Tas, J. Chin. Chem. Soc. 53 (2006) 1027.
[46] S. Chandra, R. Kumar, Spectrochim. Acta, Part. A 62 (2005) 518.
[47] S. Manjunathan, C.N. Krishnan, Asian J. Chem. 19 (2007) 861.
[48] D.N. Huh, J.B. Gibbons, R.S. Haywood, C.E. Moore, A.L. Rheingold, M.J. Ferguson, C.J.A. Daley, Inorg. Chim. Acta 423 (2014) 290.
[49] B.A. Frenz, J.A. IBers, Inorg. Chem. 11 (1972) 1109.
[50] A.K. Sharma, S. Biswas, S.K. Barman, R. Mukherjee, Inorg. Chim. Acta 363 (2010) 2720.
[51] I. García-Santos, J. Sanmartín, A.M. García-Deibe, M. Fondo, E. Gómez, Inorg. Chim. Acta 363 (2010) 193.
[52] D. Sertphon, D.J. Harding, P. Harding, H. Adams, Polyhedron 30 (2011) 2740.
[53] F. Wagner, M.T. Mocella, M.J. D'Aniello Jr., A.H.J. Wang, E. Kent, J. Am. Chem. Soc. 96 (1974) 2625.
[54] A. McAuley, C. Xu, Inorg. Chem. 31 (1992) 5549.